

# An Analytical Study of Small Unmanned Aerial Vehicle Dynamic Stability Characteristics

Abdelhakam A. Noreldien, Sakhr B. Abudarag, Muslim S. Eltoum, Salih O. Osman

**Abstract**—This paper presents an analytical study of Small Unmanned Aerial Vehicle (SUAV) dynamic stability derivatives. Simulating SUAV dynamics and analyzing its behavior at the earliest design stages is too important and more efficient design aspect. The approach suggested in this paper is using the wind tunnel experiment to collect the aerodynamic data and get the dynamic stability derivatives. AutoCAD Software was used to draw the case study (wildlife surveillance SUAV). The SUAV is scaled down to be 0.25% of the real SUAV dimensions and converted to a wind tunnel model. The model was tested in three different speeds for three different attitudes which are; pitch, roll and yaw. The wind tunnel results were then used to determine the case study stability derivative values, and hence it used to calculate the roots of the characteristic equation for both longitudinal and lateral motions. Finally, the characteristic equation roots were found and discussed in all possible cases.

**Keywords**—Model, simulating, SUAV, wind tunnel.

## I. INTRODUCTION

THE main objective of this paper is to evaluate the dynamic stability status of statically stable SUAV.

Small unmanned aerial vehicle (SUAV) is defined as a space-traversing vehicle that flies without a human crew on board and that can be remotely controlled or can fly autonomously [1].

SUAV is said to be stable, if, when on slightly disturbed from a state of equilibrium it tends to return to and remain in that state, the disturbance acting only for a finite time [2].

This paper is organized beginning with introduction section and the other sections arranged as: The 2<sup>nd</sup> section introduces the CAD drawing and model making, the 3<sup>rd</sup> section states the SUAV Axes definitions, attitudes, equations of motion and linearizing the vehicle equations of motion. The 4<sup>th</sup> section highlights the SUAV static stability (static margin) and focuses on the dynamic stability. The last section discussed the analysis of the characteristic equation roots and determination of SUAV stability status.

A road map for this paper is given in Fig. 1.

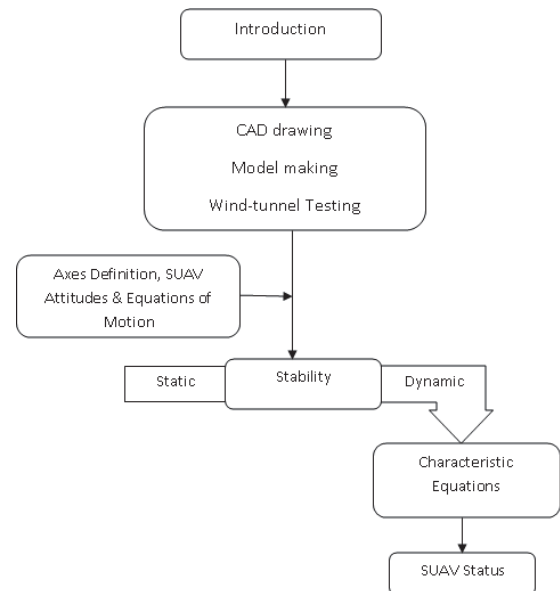


Fig. 1 Road Map

## II. CAD-DRAWING, MODEL MAKING, AND WIND-TUNNEL TESTING

### A. Cad-Drawing (Geometric Similarity)

Two geometrical objects are called similar if they both have the same shape. More precisely, one can be obtained from the other, by uniformly scaling (enlarging or shrinking), possibly with additional translation, rotation and reflection. This means that either object can be rescaled, repositioned, and reflected so as to coincide precisely with the other object.

For obtaining an analytical study of stability, the given case study must be drawn by a conventional drawing program. In this case, AutoCAD drawing program was used. The two-dimensional drawing was given in three plans (front-side-top) and the model dimensions were taken from [3]. The SUAV then converted to a three-dimension assembly drawing. The aerofoil types used on the model are NACA (2411 and 0009) for wing and tail plane respectively.

The SUAV model has been produced from a special type of light wood in order to be fitted into the wind tunnel [4]. The final model is shown in Fig. 6.

### A. Test Environment

- Altitude (above sea level, Khartoum) = 1265ft.
- Density ( $\rho$ ) = 1.177 kg/m<sup>3</sup>
- Atmospheric pressure = 1010 mbar.

Abdelhakam A. Noreldien, Sakhr B. Abudarag, Muslim S. Eltoum, Salih O. Osman are with the aeronautical Engineering Dept., Faculty of Engineering, Sudan University of Science and Technology, Sudan (phone: +249127648344, +249123083930, 249922760179, +249929027803; e-mail: hakamoov@yahoo.com, sabudarg@hotmail.com, muslimmitsu@yahoo.com, salalecho\_88@hotmail.com).

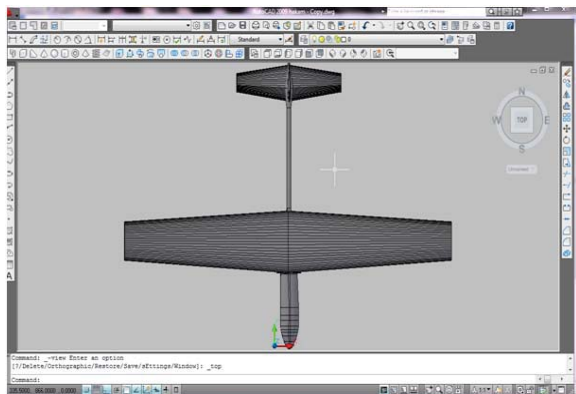


Fig. 2 Case Study Top View

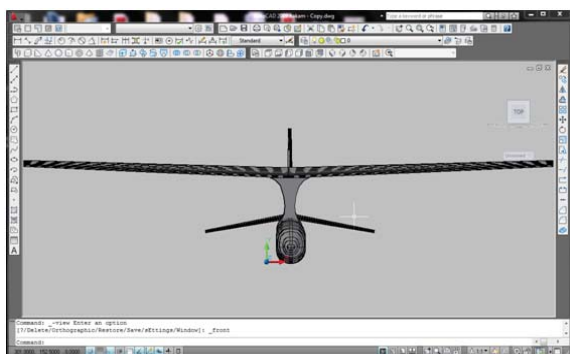


Fig. 3 Case Study Front View

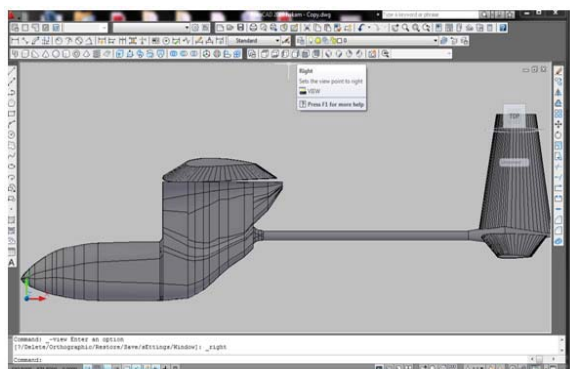


Fig. 4 Case Study Side View

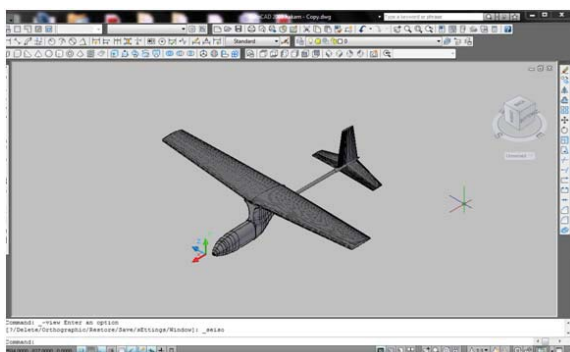


Fig. 5 Case Study 3D View



Fig. 6 Wind -Tunnel Model in Yaw Attitude

### B. Determination of Wind-Tunnel Velocity

The wind-tunnel data acquisition system which is used to calculate the velocity was a set of PITOT tube and digital pressure reading. The velocity was calculated by:

$$V = \sqrt{\frac{2 \cdot \Delta p}{\rho_a}} \quad \text{m/sec, where } \rho_a = \frac{p_a}{R \cdot t} \quad (1)$$

Table I shows three wind-tunnel velocities.

TABLE I THREE WIND-TUNNEL VELOCITIES		
Wind tunnel test-section Velocity (V)		
No	Pressure difference ( $\Delta p$ )	$V(\text{m/s}) = \sqrt{\frac{2 \cdot \Delta p}{\rho_a}}$
1	62.3642	10.325
2	61.8579	10.283
3	59.7704	10.108

### C. Dynamic Similarity

Dynamic Similarity exists between the model and the prototype when forces at corresponding points are similar. In order to obtain total similitude between model and prototype, it comes out that Reynolds number (dimensionless quantity representing the ratio of momentum forces to viscous forces) and Mach number (dimensionless quantity representing the ratio of velocity past a boundary to the local speed of sound) should be the same between the model and the prototype.

At lower speeds (Mach number 0.3 and below) it is just the Reynolds Numbers that are important and it is simply enough to preserve the Reynolds number alone. At higher speeds where compressibility is important only Mach number needs to be preserved.

### D. Reynolds Number Calculations

Three calculated result was achieved during different velocities; Reynolds number is given by:

$$R_e = \frac{\rho V L}{\mu} \quad (2)$$

At velocity (V) = 10.325 m/s:

$$R_{e1} = \frac{1.177 \cdot 10.325 \cdot 0.243}{4.1675 \times 10^{-5}} = 7.0859e + 04 .$$

At velocity (V) = 10.283 m/s:

$$R_{e_2} = \frac{1.177 * 10.283 * 0.243}{4.1675 \times 10^{-5}} = 7.0571e + 04.$$

At velocity (V) = 10.108 m/s:

$$R_{e_3} = \frac{1.177 * 10.108 * 0.243}{4.1675 \times 10^{-5}} = 6.9370e + 04.$$

#### E. Wind-Tunnel's Model Calculations

- Real wing maximum length ( $l_o$ ) = 1.8 m.
- Wind tunnel diameter (D) = 0.64 m.
- Model's wing total length ( $l_M$ ) =  $2/3 D = 2/3(0.64) = 0.43$  m.

Then, the scale factor

$$(k_l) = \frac{l_M}{l_o} = \frac{0.43}{1.8} = 0.237. \quad (3)$$

Density scale

$$(k_\rho) = \frac{\rho_{tunnel}}{\rho_{light}} = \frac{1.176}{1.173} = 1.003. \quad (4)$$

Model mass scale

$$k_m = k_\rho k_l^3. \quad k_m = 1.003 * (0.237)^3 = 0.0133. \quad (5)$$

So,

$$\text{Mass of the model} = (\text{Real mass} * 0.0133) = (3.371 * 0.0133) = 0.045 \text{ kg}. \quad (6)$$

Equations (3)-(6) were taken from [5].

#### F. Wind-Tunnel Test Experiment

The SUAV model was set up in the wind tunnel to be tested precisely. The output results from testing the model were taken from three-component balance display unit shown in Fig. 7. The test is aiming to produce approximate values of

Lift, Drag and Moment corresponding SUAV. The experiment was done in three phases:

*First:* The model was adjusted to pitch attitude, Fig. 9. Readings were taken from different velocities which were multiplied by 70% (V= 10.325, 10.283 and 10.108 m/s) respectively, in different angles of attack, ( $\alpha = -3, 0, 3, 6, 9, 12$  and  $15^\circ$ ) for each speed.

The Actual wind tunnel velocities were adjusted to 70% to avoid the possible inaccuracy in both wind tunnel and the model.

*Secondly:* In similar manner for yawing attitude, Fig. 6, reading was also taken from three different velocities (V= 10.325, 10.283 and 10.108 m/s) respectively, but in angles of attack ( $\alpha = 0, 3, 6, \text{ and } 9^\circ$ ) for each speed.

*Finally:* For rolling attitude, readings were taken for speed of 9 m/s at angles of attack equal to ( $\alpha = 5, 10, 15$  and  $20^\circ$ ).



Fig. 7 Three-Component Balance Display Unit

#### G. Wind-Tunnel Test Experiment Results

The following tables show the results of wind-tunnel test for pitch, yaw and roll attitude. The lift and drag were taken in the units of the gram force.

The moment was taken in gram force times millimeter

TABLE II  
AT SPEED (V) = 10.325 M/S (PITCH ATTITUDE)

A	L	D	M	CL	CD	CM	L/D
-3	-123	9	-0.0044	-0.00931	0.000681489	-6.34614E-09	-13.6667
0	175	45	-0.005	0.013251	0.003407445	-7.21152E-09	3.888889
3	223	83	-0.017	0.016886	0.006284843	-2.45192E-08	2.686747
6	245	97	-0.037	0.018552	0.007344938	-5.33653E-08	2.525773
9	263	125	-0.039	0.019915	0.009465126	-5.62499E-08	2.104
12	266	164	-0.04	0.020142	0.012418245	-5.76922E-08	1.621951
15	162	172	-0.044	0.012267	0.013024013	-6.34614E-08	0.94186

TABLE III  
AT SPEED (V) = 10.283 M/S (PITCH ATTITUDE)

A	L	D	M	CL	CD	CM	L/D
-3	-95	3	-0.029	-0.00719	0.000227	-4.18268E-08	-31.6667
0	165	24	-0.033	0.012494	0.001817	-4.75961E-08	6.875
3	219	66	-0.034	0.016583	0.004998	-4.90384E-08	3.318182
6	249	86	-0.036	0.018855	0.006512	-5.1923E-08	2.895349
9	259	104	-0.044	0.019612	0.007875	-6.34614E-08	2.490385
12	298	153	-0.047	0.022565	0.011585	-6.77883E-08	1.947712
15	151	158	-0.053	0.011434	0.011964	-7.64422E-08	0.955696

TABLE IV  
AT SPEED (V) = 10.108 M/S (PITCH ATTITUDE)

A	L	D	M	CL	CD	CM	L/D
-3	-86	1	-0.027	-0.00651	7.5721E-05	-3.89422E-08	-86
0	167	16	-0.03	0.012645	0.00121154	-4.32691E-08	10.4375
3	190	49	-0.031	0.014387	0.00371033	-4.47115E-08	3.877551
6	204	94	-0.044	0.015447	0.00711777	-6.34614E-08	2.170213
9	257	103	-0.054	0.01946	0.00779926	-7.78845E-08	2.495146
12	266	144	-0.059	0.020142	0.01090382	-8.5096E-08	1.847222
15	102	156	-0.067	0.007724	0.01181248	-9.66344E-08	0.653846

TABLE V  
AT SPEED (V) = 10.325 M/S (YAW ATTITUDE)

A	L	D	M	CL	CD	CM	L/D
0	2	1	-0.001	0.000151	7.5721E-05	-1.4423E-09	10.4375
3	3	2	-0.003	0.000227	0.000151442	-4.32691E-09	3.877551
6	4	3	-0.007	0.000303	0.000227163	-1.00961E-08	2.170213
9	18	5	-0.009	0.001363	0.000378605	-1.29807E-08	2.495146

TABLE VI  
AT SPEED (V) = 10.283 M/S (YAW ATTITUDE)

A	L	D	M	CL	CD	CM	L/D
0	5	12	-0.003	0.000379	0.000909	-4.32691E-09	10.4375
3	19	14	-0.006	0.001439	0.00106	-8.65383E-09	3.877551
6	28	18	-0.007	0.00212	0.001363	-1.00961E-08	2.170213
9	64	19	-0.009	0.004846	0.001439	-1.29807E-08	2.495146

TABLE VII  
AT SPEED (V) = 10.108 M/S (YAW ATTITUDE)

A	L	D	M	CL	CD	CM	L/D
0	2	8	-0.001	0.000151	0.00060577	-1.4423E-09	10.4375
3	3	26	-0.003	0.000227	0.00196875	-4.32691E-09	3.877551
6	18	31	-0.004	0.001363	0.00234735	-5.76922E-09	2.170213
9	36	36	-0.005	0.002726	0.00272596	-7.21152E-09	2.495146

TABLE VIII  
AT SPEED (V) = 9 M/S (ROLL ATTITUDE)

A	L	D	M	CL	CD	CM	L/D
5	5	1.25	-0.02	0.000378605	9.47E-05	-2.9E-08	4
10	14	1.3	-0.03	0.001060094	9.84E-05	-4.3E-08	10.76923
15	18	2	-0.07	0.001362978	0.000151	-1E-07	9
20	24	2.1	-0.01	0.001817304	0.000159	-1.4E-08	11.42857

### III. XES DEFINITION, ATTITUDES, AND EQUATIONS OF MOTION

#### A. Axes Definitions

Reference [6] shows that the position (and hence motion) of the SUAV is generally defined relative to one of three sets of co-ordinate systems:

##### 1. Wind Axes

- **X Axis** - Positive in the direction of the oncoming air (relative wind).
- **Y Axis** - Positive Right to X Axis, perpendicular to X Axis.
- **Z Axis** - Positive downwards, perpendicular to X-Y plane.

##### 2. Inertial Axes (or Body Axes)

Based about SUAV Centre of Gravity (CG) as follow:

- **X Axis** - Positive forward, through nose of SUAV
- **Y Axis** - Positive to Right of X Axis, perpendicular to X Axis.
- **Z Axis** - Positive downwards, perpendicular to X-Y plane.

##### 3. Earth Axes

- **X Axis** - Positive in the direction of North.
- **Y Axis** - Positive in the direction of East (perpendicular to X Axis).
- **Z Axis** - Positive towards the centre of Earth (perpendicular to X-Y Plane).

#### B. SUAV Attitude

Consider a coordinate system xyz, aligned having x pointing in the direction of true north, y pointing to true east, and the z-axis pointing down, normal to the local horizontal direction. Given this setting, the rotation sequence from xyz to

XYZ is specified by and it defines the angles yaw, pitch and roll as:

- Righthanded rotation  $\psi \in (-180,180)$ : About the z-axis by the yaw angle
- rotation  $\theta \in (-90,90)$ : About the new (once- rotated) y-axis by the pitch angle
- rotation  $\phi \in (-180,180)$ : About the new (twice-rotated) x-axis by the roll angle

Fig. 7 shows the attitude angles Yaw, pitch and roll angles. Fixed frame xyz has been moved backwards from center of gravity (preserving angles) for clarity. Axes Y and Z are not shown.

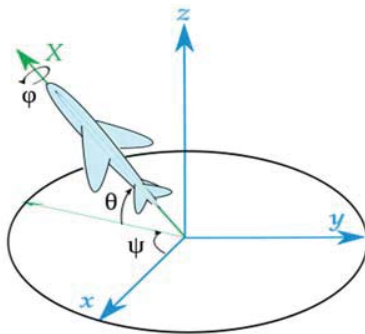


Fig. 8 Yaw, Pitch and Roll Angles



Fig. 9 Pitch Attitude



Fig. 10 Roll Attitude

### C. The SUAV Equations of Motion

The equations of motion used in this work are derived from [7]

$$\sum M = \frac{dH}{dt} = \frac{d}{dt}(H) \quad (7)$$

$$\sum F_o + \Delta F = m \frac{dm}{dt} V_T + m \frac{dV_T}{dt} \quad (8)$$

$$\sum \Delta F = m \frac{dV_T}{dt} \quad (9)$$

$$\frac{dV_T}{dt} = \frac{dV_T}{dt} + \omega * V_T.$$

$$\left. \begin{aligned} V_T &= iu + jv + kw \\ \omega &= iP + jQ + kR \end{aligned} \right\} \quad (10)$$

By cross-multiplying:

$$\omega \times V_T = \begin{vmatrix} i & j & k \\ P & Q & R \\ u & v & w \end{vmatrix} = i(Qw - vR) + j(Ru - Pw) + k(Pv - Qu). \quad (11)$$

Also:

$$\sum \Delta F = i \sum \Delta F_x + j \sum \Delta F_y + k \sum \Delta F_z. \quad (12)$$

And from (10)

$$\frac{d}{dt} V_T = i\dot{u} + j\dot{v} + k\dot{w}.$$

Then:

$$\left. \begin{aligned} \sum \Delta F_x &= m * (\dot{u} + wQ - vR) \\ \sum \Delta F_y &= m * (\dot{v} + uR - wP) \\ \sum \Delta F_z &= m * (\dot{w} + vP - uQ) \end{aligned} \right\} \quad (13)$$

These three equations are the force equations.

Moment: To obtain the equations of angular motion, it is necessary to return to (7), which is repeated here:

$$\sum M = \frac{dH}{dt}.$$

The tangential velocity can be expressed by the vector cross product as:

$$V_{tan} = \omega \times R. \quad (14)$$

Then the incremental momentum resulting from this tangential velocity of the element of mass can be expressed as:  $dM = (\omega \times R)dm$ .

The moment of momentum is the momentum times the lever arm or, as a vector equation,

$$dH = r \times (\omega \times R) dm. \quad (15)$$

$$H = \int r \times (\omega \times R) dm. \quad (16)$$

In evaluating the triple cross product if  $\omega = iP + jQ + kR$  and  $r = ix + jy + kz$ . Then:



$$\omega \times R = \begin{vmatrix} i & j & k \\ P & Q & R \\ x & y & z \end{vmatrix} \quad (17)$$

Expanding:

$$\begin{aligned} \omega \times R &= i(Qz - Ry) + j(xR - Pz) + k(Py - xQ) \\ r \times (\omega \times R) &= \begin{vmatrix} i & j & k \\ x & y & z \\ Qz - Ry & xR - Pz & Py - xQ \end{vmatrix} \end{aligned} \quad (18)$$

Expanding:

$$r \times (\omega \times R) = i[(y^2 + z^2)P - xyQ - xzR] + j[(z^2 + x^2)Q - yzR - xyP] + k[(x^2 + y^2)R - xzP - yzQ] \quad (19)$$

Substituting (19) into (16), it becomes

$$H = \int i[(y^2 + z^2)P - xyQ - xzR]dm + \int j[(z^2 + x^2)Q - yzR - xyP]dm + \int k[(x^2 + y^2)R - xzP - yzQ]dm \quad (20)$$

From the first assumption that (20) can be written component from as:

$$\left. \begin{aligned} H_x &= PI_x - RJ_{xz} \\ H_y &= QI_y \\ H_z &= RI_z - PJ_{xz} \end{aligned} \right\} \quad (21)$$

As the SUAV is assumed to be rigid body of constant mass, the time rates of change of the moments and product of inertia are zero, now:

$$\omega \times H = \begin{vmatrix} i & j & k \\ P & Q & R \\ H_x & H_y & H_z \end{vmatrix} \quad (22)$$

Expanding:

$$\omega \times H = i(QH_z - RH_y) + j(H_xR - PH_z) + k(PH_y - QH_x) \quad (23)$$

$$\sum \Delta M = i \sum \Delta L + j \sum \Delta M + k \sum \Delta N \quad (24)$$

By equating components of (23), (24) and substituting  $H_x$ ,  $H_y$  and  $H_z$  from (13) the angular equations of motion are obtained:

$$\left. \begin{aligned} \sum \Delta L &= \dot{P}I_x - \dot{R}J_{xz} + QR(I_z - I_y) - PQJ_{xz} \\ \sum \Delta M &= \dot{Q}I_y + PR(I_x - I_z) + (P^2 - R^2)J_{xz} \\ \sum \Delta N &= \dot{R}I_z - \dot{P}J_{xz} + \dot{Q}(I_y - I_x) + QRJ_{xz} \end{aligned} \right\} \quad (25)$$

*D. Linearizing and Separation of the Equation of Motion*

A study of (13) and (24) shows that it takes six simultaneous non-linear equations of motion to completely describe the behavior of rigid SUAV. References [6], [8] show the linearization process.

#### IV. STABILITY

##### A. Static Stability

All SUAV stability equations are derived from [7].

$$\text{Static margin}(k_n) = -\left(\frac{\partial C_m}{\partial C_L}\right) = (h_n - h). \quad (25)$$

$$k_n = h_{n\bar{c}} - h_{o\bar{c}} = 0.64.$$

$$h_n = h_{n\bar{c}} + \bar{v} \frac{a_1}{a} \left(1 - \frac{\partial \epsilon}{\partial \alpha}\right) = 1.03, \quad h_{o\bar{c}} < h_n. \quad (26)$$

##### B. Dynamic Stability

Total efficiency of propulsion system equation was taken from [3]-[9]. As the case study is electrical powered then

$$\eta_{\text{propulsion}} = \eta_{\text{prop}} * \eta_{\text{esc}} * \eta_{\text{battery}} = 0.53. \quad (27)$$

Average velocity:

$$V_{\text{avg1}} = \eta_{\text{prop}} \left[ \frac{2 P_{\text{max output}}}{\pi \rho_{\text{alt}} D^2 (1 - \eta_{\text{prop}})} \right]^{\frac{1}{3}} = 10.5 \frac{\text{m}}{\text{s}}. \quad (28)$$

$$P_{\text{max}} = P_{\text{min}} * \eta_{\text{esc}} * \eta_{\text{motor}}.$$

Engine Thrust:

$$Th_1 = \frac{P_{\text{max output}} * \eta_{\text{total}}}{V_{\text{avg}}} = 14.2 \text{ N}. \quad (29)$$

In similar manner,  $V_{\text{avg2}}$  and  $Th_2$  equal to 11.40 and 16.85 respectively. Then the thrust rate to velocity  $\left(\frac{\partial T}{\partial v}\right)$  is obtained accordingly.

##### 1. Longitudinal Aerodynamic Derivatives

- X-force component:

$$\widehat{X}_u = -2C_D - V_e \frac{\partial C_D}{\partial v} + \frac{1}{0.5\rho V_e S} \frac{\partial T}{\partial v} = 30.14. \quad (30)$$

$$\widehat{X}_w = C_L - \frac{\partial C_D}{\partial \alpha} = 0.0158. \quad (31)$$

- Z-Force component:

$$\widehat{Z}_u = -2C_L - V_e \frac{\partial C_L}{\partial v} = -0.2652. \quad (32)$$

$$\widehat{Z}_w = -\left(C_D + \frac{\partial C_L}{\partial \alpha}\right) = -0.0064. \quad (33)$$

$$\widehat{Z}_{q(\text{tail})} = -a_1 \bar{V}_T = -0.0009. \quad (34)$$

$$\widehat{Z}_w = \widehat{Z}_{q(\text{tail})} * \frac{\partial \epsilon}{\partial \alpha} = -0.00001. \quad (35)$$

- Pitching moment:

$$\text{At low speed } \widehat{M}_u = 0. \quad (36)$$

$$\widehat{M}_w = -\left(\frac{\partial C_L}{\partial \alpha}\right) * k_n = -8.9600e - 04. \quad (37)$$

$$\overline{M_{q(\text{tail})}} = \left( \overline{l_T / \bar{c}} \right) * \overline{Z_{q(\text{tail})}} = -0.03567. \quad (38)$$

$$\overline{M_{q(\text{wing})}} = \frac{1}{2} C_{m_q} = -0.235. \quad (39)$$

$$\overline{M_q} = \overline{M_{q(\text{wing})}} + \overline{M_{q(\text{tail})}} = -0.2706. \quad (40)$$

## 2. Lateral Aerodynamic Derivatives

- Rolling moment derivative due to sideslip: Contribution of wing dihedral:

$$L_{v_{\text{wing}}} = -0.2C_L = -0.0332. \quad (41)$$

$$L_{v_{\text{fin}}} = -a\bar{V}_f \frac{h_f}{l_f} = -3.3049e - 08. \quad (42)$$

$$L_{v_{\text{fuselage}}} = 0.$$

$$L_v = L_{v_{\text{fuselage}}} + L_{v_{\text{wing}}} + L_{v_{\text{fin}}} = -0.0332. \quad (43)$$

- Rolling moment derivative due to rate of roll: Contribution of wing:

$$\widehat{L_p} = -\frac{1}{2Ss^2} \int_0^s (C_D + \frac{\partial C_L}{\partial \alpha}) cy^2 dy = -7.4e - 5. \quad (44)$$

The contribution of fuselage and fin are neglected.

- Rolling moment derivative due to rate of yaw:

$$\overline{L_r(\text{wing})} = \frac{1}{Ss^2} \int_0^s (C_L)_1 cy^2 dy = 0.0018. \quad (45)$$

$$\overline{L_r(\text{fin})} = -a_1 \bar{V}_f \frac{h_f}{b} = -3.3049e - 08. \quad (46)$$

- Yawing moment derivatives due to sideslip:

$$N_{v(\text{fuselage})} = \frac{s_B l_B}{Sb} n_B = -0.521. \quad (47)$$

$$N_B = -0.1. \quad (48)$$

$$N_{v(\text{fin})} = a_1 \bar{V}_f = 2.2400e - 06.$$

$$N_v = N_{v(\text{fuselage})} + N_{v(\text{fin})} = -0.521. \quad (49)$$

- Yawing moment derivatives due to rate of roll:

$$N_p = -\frac{1}{2Ss^2} \int_0^s (C_L - \frac{\partial C_D}{\partial \alpha}) cy^2 dy = -0.00019. \quad (50)$$

- Yawing moment derivatives due to rate of yaw:

$$\overline{N_r(\text{wing})} = -\frac{1}{Ss^2} \int_0^s (C_D)_1 cy^2 dy = 0.00053. \quad (51)$$

$$\overline{N_r(\text{fin})} = \frac{l_f}{b} N_{v(\text{fin})} = -0.0137. \quad (52)$$

$$\overline{N_r(\text{total})} = \overline{N_r(\text{wing})} + \overline{N_r(\text{fin})} = 0.00053. \quad (53)$$

- Side force derivative due to sideslip:

$$Y_{v(\text{fuselage})} = \frac{s_B}{S} y_B = -0.7878. \quad (54)$$

$$y_B = -0.1. \quad (55)$$

$$Y_{v(\text{fin})} = a_1 \frac{S_f}{S} = -0.000014. \quad (56)$$

$$Y_{v(\text{total})} = Y_{v(\text{fuselage})} + Y_{v(\text{fin})} = -0.789. \quad (57)$$

## 3. Dynamic Stability Characteristics

Consider a horizontal flight  $\theta_e = 0$

$$\tau = \frac{m}{0.5\rho_e V_e S} = 0.59. \quad (58)$$

$$\mu_1 = \frac{m}{0.5\rho_e S \bar{c}} = 53.4. \quad (59)$$

$$\mu_2 = \frac{m}{0.5\rho_e S b} = 7.21. \quad (60)$$

$$i_x = \frac{I_x}{mb} = 0.25. \quad (61)$$

$$i_y = \frac{I_y}{m\bar{c}^2} = 32.87. \quad (62)$$

$$i_z = \frac{I_z}{mb^2} = 0.5. \quad (63)$$

$$i_{zx} = \frac{I_{zx}}{mb^2} = 0.05. \quad (64)$$

$$\hat{g}_1 = C_L = 0.0166. \quad (65)$$

$$\hat{g}_2 = C_L \tan \theta_e = 0.0008. \quad (66)$$

- Longitudinal Characteristics

From [7], it is found that:

$$\begin{vmatrix} \lambda + x_u & x_w \lambda + x_w & x_q \lambda + \hat{g}_1 \\ z_u & (1 + z_w) \lambda + z_w & (z_q - 1) \lambda + \hat{g}_2 \\ m_u & m_w \lambda + m_w & m_w \lambda + m_w \end{vmatrix} = 0.$$

So the characteristic equation is:

$$A_1 \lambda^4 + B_1 \lambda^3 + C_1 \lambda^2 + D_1 \lambda^1 + E_1. \quad (67)$$

where:

$$A_1 = 1 + z_w.$$

$$B_1 = x_u A_1 + z_w - x_w z_u + A_\delta m_q + (1 - z_q) m_w$$

$$C_1 = x_u z_w - x_w z_u + [x_u A_\delta + z_w - x_w z_u] m_q + [x_u (1 - z_q) + x_q z_u - \hat{g}_2] m_w + (1 - z_q) m_w - [x_w (1 - z_q) + x_q A_\delta] m_q.$$

$$D_1 = (x_u z_w - x_w z_u) m_q + (\hat{g}_1 z_u - \hat{g}_2 x_u) m_w + [x_u (1 - z_q) + x_q z_u - \hat{g}_2] m_w - [x_w (1 - z_q) + z_q z_w + \hat{g}_1 A_\delta - \hat{g}_2 x_w] m_u.$$

$$E_1 = (\hat{g}_1 z_u - \hat{g}_2 x_u) m_w - (\hat{g}_1 z_w - \hat{g}_2 x_w) m_u.$$

$$x_i = -\widehat{X}_u = -30.14. \quad (68)$$

$$x_w = -\widehat{X}_w = -0.0158. \quad (69)$$

$$x_w = \hat{x}_q = 0. \quad (70)$$

$$z_u = -\hat{z}_u = 0.2652. \quad (71)$$

$$z_w = -\hat{z}_w = 0.0064. \quad (72)$$

$$z_{\dot{w}} = -\frac{\hat{z}_w}{\mu_1} = -0.0001199. \quad (73)$$

$$z_q = -\frac{\hat{z}_q}{\mu_1} = 0.0000196. \quad (74)$$

$$m_u = 0. \quad (75)$$

$$m_w = -\mu_1 \frac{M_w}{i_y} = 0.0001442. \quad (76)$$

$$m_{\dot{w}} = -\frac{M_w}{i_y} = 0.0000273. \quad (77)$$

$$m_q = -\frac{M_q}{i_y} = 0.0082. \quad (78)$$

$$m_w = -\mu_1 \frac{M_w}{i_y} = 0.00041. \quad (79)$$

Thus:

$$A_1 = 0.9936, B_1 = 29.6842, C_1 = -8.2905, D_1 = 0.0240, E_1 = 0.0000274.$$

and

$$\Delta\lambda = 0.9936\lambda^4 + 29.6842\lambda^3 + -8.2905\lambda^2 + 0.0240\lambda^1 + 0.0000274$$

The roots of the characteristic equation for longitudinal dynamic stability are:

$$\lambda_1 = -30.1521, \lambda_2 = 0.2738, \lambda_3 = 0.0038, \lambda_4 = -0.0009.$$

#### • Lateral Characteristics

Also from [7], it is found that:

$$\begin{vmatrix} \lambda + y_v & y_p\lambda - \hat{g}'_1 & (1 - y_r\lambda) - \hat{g}_2 \\ l_v & \lambda^2 + l_p\lambda & e_x\lambda^2 + l_r\lambda \\ n_v & e_z\lambda^2 + n_p\lambda & \lambda^2 + n_r\lambda \end{vmatrix} = 0.$$

So the characteristic equation is:

$$A_2\lambda^5 - B_2\lambda^4 + C_2\lambda^3 + D_2\lambda^2 + E_2\lambda = 0. \quad (80)$$

where:

$$A_2 = 1 - e_x e_z.$$

$$B_2 = l_p + n_r - e_x n_p - e_z l_r + A_2 y_v.$$

$$C_2 = l_p n_r - l_r n_p + [l_p + n_r - e_x n_p - e_z l_r] y_v + [e_x(1 + y_r) - y_p] l_v - [1 + y_r - e_x y_p] n_v.$$

$$D_2 = (l_p n_r - l_r n_p) y_v + [n_p(1 + y_r) - n_r y_p + \hat{g}_1 - e_z \hat{g}_2] l_v [l_p(1 + y_r) - l_r y_p - \hat{g}_2 + e_x \hat{g}_1] n_v.$$

$$E_2 = (\hat{g}_1 n_r - \hat{g}_2 n_p) l_v - (\hat{g}_1 l_r - \hat{g}_2 l_p) n_v.$$

$$y_p = y_r = 0.$$

$$y_v = -Y_v = 0.7.$$

$$l_v = -\frac{\mu_2 L_v}{i_x} = 0.96.$$

$$l_p = -\frac{\hat{L}_p}{i_x} = 0.000296.$$

$$l_r = -\frac{\hat{L}_r}{i_x} = -0.0018$$

$$n_v = -\frac{\mu_2 N_v}{i_z} = 7.51.$$

$$n_p = -\frac{N_p}{i_z} = 0.00038.$$

$$n_r = -\frac{N_r}{i_z} = 0.011.$$

$$e_x = -\frac{i_{zx}}{i_x} = -2.24.$$

$$e_z = -\frac{i_{zx}}{i_z} = 1.12.$$

Thus:

$$A_2 = 3.5088, B_2 = 2.7470, C_2 = 0.0673, D_2 = 0.0042, E_2 = 0.0002138.$$

$$\Delta(\lambda) = 3.5088\lambda^4 + 2.7470\lambda^3 + 0.0673\lambda^2 + 0.0042\lambda^1 + 0.0002138 = 0.$$

#### V. ANALYSIS OF THE CHARACTERISTICS EQUATION ROOTS (SUAV STATUS)

Fig. 11 from [7] shows the roots of the characteristic equation behavior and hence the SUAV stability states.

**Divergence:** When  $\lambda$  is real and positive, the constituent ( $\hat{u}$ ,  $\hat{w}$  and  $\theta$  or their derivatives to respect to  $\hat{t}$ ) of the disturbed motion increase stability with time and tends to infinity.

**Subsidence:** When  $\lambda$  is real and negative, the constituent decreases with time, ending asymptotically to zero. When  $\lambda$  is complex, it can be written as:

$$\lambda = -r + is$$

where  $r$  and  $s$  are real. Now the coefficients occurring in the characteristic equation are real constants, and thus the equation will have another root:

$$\lambda = -r - is.$$

the two modes corresponding to the roots  $-r + is$  can be combined to give:

$$\hat{u} = \sigma_1 e^{-r\hat{t}} \cos s\hat{t} + \sigma_2 e^{-r\hat{t}} \sin s\hat{t}$$



where  $\sigma_1$  and  $\sigma_2$  are real constants, and similarly for  $\hat{w}$  and  $\theta$ .

When  $r$  is positive, the constituent of the disturbed motion is *Damped Oscillation*, tending to zero.

Increasing Oscillation: When  $r$  is negative, the constituent of the disturbed motion is tending to  $\pm\infty$  as  $\hat{t} \rightarrow \infty$ .

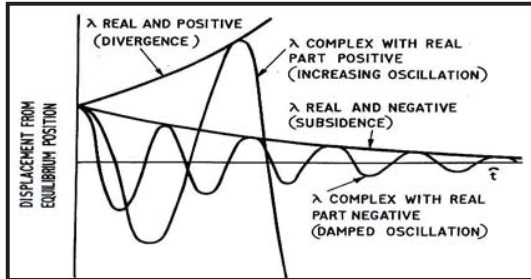


Fig. 11 Types of Motion Corresponding to the Roots of the Characteristics Equation [7]

#### A. For Longitudinal Dynamic Stability

The roots of the characteristic equation for longitudinal dynamic stability are:

$$\lambda_1 = -30.1521.$$

$$\lambda_2 = 0.2738.$$

$$\lambda_3 = 0.0038.$$

$$\lambda_4 = -0.0009.$$

The characteristic equation has four real roots two of the real roots having a negative real part.

#### • Damping for Longitudinal Motion

The large negative root corresponds to the heavily damped rolling subsidence. The time  $t_{\frac{1}{2}}$  to half-amplitude is:

$$\tau = v \cdot cl / (g^* \cos(A)) = 0.0174$$

$$t_{\frac{1}{2}} = \frac{\ln 2}{|\lambda_1|} * \tau = \frac{\ln 2}{30.1521} * (0.0174) = 0.0004 \text{ sec} \quad (81)$$

#### • Period for Longitudinal Motion:

The small negative root corresponds to lightly damped spiral subsidence, the time  $t_{\frac{1}{2}}$  to half-amplitude is:

$$t_{\frac{1}{2}} = \frac{\ln 2}{|\lambda_4|} * \tau = \frac{\ln 2}{0.0009} * (0.0174) = 13.45 \text{ sec}$$

#### B. For Lateral Dynamic Stability

The roots of the characteristic equation for longitudinal dynamic stability are:

$$\lambda_1 = -0.7596 + 0.0000i.$$

$$\lambda_2 = 0.0077 + 0.0449i.$$

$$\lambda_3 = 0.0077 - 0.0449i.$$

$$\lambda_4 = -0.0387 + 0.0000i.$$

The characteristic equation has two real roots and a pair of complex roots, the real roots having a negative real part.

#### • Period for Longitudinal Motion:

The large negative root corresponds to the heavily damped rolling subsidence. The time  $t_{\frac{1}{2}}$  to half-amplitude is:

$$t_{\frac{1}{2}} = \frac{\ln 2}{|\lambda_2|} * \tau = \frac{\ln 2}{0.7596} * (0.0174) = 0.0159 \text{ sec.}$$

#### • Damping for Longitudinal Motion

The small negative root corresponds to lightly damped spiral subsidence, the time  $t_{\frac{1}{2}}$  to half-amplitude is:

$$t_{\frac{1}{2}} = \frac{\ln 2}{|\lambda_1|} * \tau = \frac{\ln 2}{0.0387} * (0.0174) = 0.312 \text{ sec.}$$

The period  $T$  is:

$$T = \frac{2\pi}{s} \tau = 2.443 \text{ sec.}$$

#### VI. CONCLUSION

The following conclusions have been drawn from the work presented here:

For longitudinal motion, it is found that the characteristic equation has two negative real roots. This means that the SUAV is in subsidence state, while the other two positive roots indicate that it is in Divergence state. For lateral motion it found that the characteristic equation has two complex roots one of them has real part negative and this indicates that the damped oscillation was achieved and the other positive real part indicate the SUAV state is increasing in oscillation.

The other pair of roots is real and negatives and this indicates that subsidence state was achieved.

#### NOMENCLATURE

symbol	Description
$A$	Taper Ratio
$AR$	Aspect Ratio
$b$	Wing Span
$C_{mean}$	Mean chord length
$D$	Drag force
$\Delta F_x$	Force component along X axis
$\Delta f$	Small disturbance in force
$H$	Angular momentum
$H_x$	Angular moment component along x axis
$H_y$	Angular moment component along y axis
$H_z$	Angular moment component along z axis
$HST$	Horizontal stabilizer area
$I_x$	Moment of inertia about X axis
$I_y$	Moment of inertia about Y axis
$i_t$	Tail incidence angle
$i_w$	Wing incidence angle
$L_p$	Dimensional rolling moment derivative due rate of roll
$L_T$	Rolling moment due to propulsion
$L_w$	Lift of wing
$L_t$	Lift of tail
$M$	Moment
$M_q$	Dimensional pitching moment derivative rate of pitch

$M_T$	Pitching moment due to propulsion
$M_t$	Tail moment
$M_w$	Dimensional pitching moment derivative velocity increment along O-Z
$M_\alpha$	Dimensional pitching moment derivative due angle of attack
$M_{\dot{w}}$	Dimensional pitching moment derivative due rate of change in velocity along O-Z
$N_r$	Dimensional yawing moment derivative due to rate of yaw
$N_T$	yaw moment due to propulsion
$N_{\delta_a}$	Dimensional yawing moment derivative due aileron deflection
$N_{\delta_r}$	Dimensional yawing moment derivative due to rudder deflection
$P$	Air density
$U$	Velocity component along x axis
$V$	Velocity component along y axis
$W$	Velocity component along z axis
$XAC$	Aerodynamic Centre location
$X_{NP}$	Neutral point location
$X_u$	Dimensional force derivative due velocity along x axis
$X_w$	Dimensional force derivative due velocity increment along O-Z
$X_{\delta_e}$	Dimensional force derivative due elevator deflection
$x_T$	Propulsive forces in x axis
$Y_T$	Propulsive forces in y axis
$Y_\beta$	Dimensional force derivative due to side slip
$Z_T$	Propulsive forces in z axis
$Z_u$	Dimensional force derivative due velocity along Z axis
$Z_{\delta_e}$	Dimensional force derivative due elevator deflection
$\theta_e, \alpha$	Angle of attack
$\alpha_t$	Tail angle of attack
$\alpha_w$	Wing angle of attach
$\Delta\delta_a$	Aileron deflection
$\Delta\delta_r$	rudder deflection
$\Delta\delta_e$	Elevator deflection
$\eta$	Tail plane efficiency
$\lambda$	Root of characteristic equation
$\omega$	Angular velocity
$\frac{\partial C_D}{\partial \alpha}$	Variation of drag coefficient with angle of attack
$\frac{\partial C_D}{\partial v}$	Variation of drag coefficient with velocity
$\frac{\partial C_L}{\partial \alpha}$	Variation of lift coefficient with velocity
$0.9 \frac{\partial c_l}{\partial \alpha}$	Lift curve slope of the wing (a)
$0.1 \frac{\partial c_l}{\partial \alpha}$	Lift curve slope of the tail plane
$\frac{\partial T}{\partial v}$	Variation of thrust with UAV velocity
$\frac{\partial \varepsilon}{\partial \alpha}$	Variation of downwash to a angle of attack

- [9] Shinar, J., *Performance, stability, dynamics and control of airplanes: Bandu N. Pamadi; AIAA Educational Series, New York, 1998, ISBN 1-56347-222-8*. 2001, Pergamon press.

## REFERENCES

- [1] R. Yanushevsky, *Guidance of Unmanned Aerial Vehicles* (CRC Press, 2011).
- [2] Cook, Michael V *Flight dynamics principles: a linear systems approach to aircraft stability and control*, 2012. Butterworth-Heinemann.
- [3] Lee, K., *Development of unmanned aerial vehicle (UAV) for wildlife surveillance*. 2004, University of Florida.
- [4] Rae, W.H. and A. Pope, *Low-speed wind tunnel testing*. 1984: John Wiley.
- [5] Alroface, K.H., *Aeroelasticity* 2007, Sudan: Sudan University of Science and Technology.
- [6] Blakelock, J.H., *Automatic control of aircraft and missiles*. 1991: John Wiley & Sons.
- [7] Babister, A.W., *Aircraft Dynamic Stability and Response: Pergamon International Library of Science, Technology, Engineering and Social Studies*. 2013: Elsevier.
- [8] Ahmed, A. E.; Hafez, A.; Ouda, A.; Ahmed, H. E. H.; ABD-Elkader, H. M., *Modeling of a Small Unmanned Aerial Vehicle*, 2015 Journal article.